Coral Reefs (2015) 34:249–257
DOI 10.1007/s00338-014-1218-2

REPORT

Porites white patch syndrome: associated viruses and disease physiology

S. A. Lawrence · J. E. Davy · W. H. Wilson · O. Hoegh-Guldberg · S. K. Davy

Received: 10 April 2014 / Accepted: 19 September 2014 / Published online: 30 September 2014

Abstract In recent decades, coral reefs worldwide have undergone significant changes in response to various environmental and anthropogenic impacts. Among the numerous causes of reef degradation, coral disease is one factor that is to a large extent still poorly understood. Here, we characterize the physiology of white patch syndrome (WPS), a disease affecting poritid corals on the Great Barrier Reef. WPS manifests as small, generally discrete patches of tissue discolouration. Physiological analysis revealed that chlorophyll *a* content was significantly lower in lesions than in healthy tissues, while host protein content remained constant, suggesting that host tissue is not affected by WPS. This was confirmed by transmission electron microscope (TEM) examination, which showed intact host tissue within lesions. TEM also revealed that *Symbiodinium* cells are lost from the host gastrodermis with no apparent harm caused to the surrounding host tissue. Also present in the electron micrographs were numerous virus-like particles (VLPs), in both coral and *Symbiodinium* cells. Small (<50 nm diameter) icosahedral VLPs were significantly more abundant in coral tissue taken from diseased colonies, and there was an apparent, but not statistically significant, increase in abundance of filamentous VLPs in *Symbiodinium* cells from diseased colonies. There was no apparent increase in prokaryotic or eukaryotic microbial abundance in diseased colonies. Taken together, these results suggest that viruses infecting the coral and/or its resident *Symbiodinium* cells may be the causative agents of WPS.

Keywords *Porites lobata* · *Porites lutea* · *Porites australiensis* · Coral disease · Virus

Communicated by Handling Editor Anastazia Banaszak

Electronic supplementary material The online version of this article (doi:10.1007/s00338-014-1218-2) contains supplementary material, which is available to authorized users.

S. A. Lawrence · J. E. Davy · S. K. Davy (✉)
School of Biological Sciences, Victoria University of Wellington, PO Box 600, Wellington, New Zealand
e-mail: simon.davy@vuw.ac.nz

W. H. Wilson
Plymouth Marine Laboratory, Prospect Place, The Hoe, Plymouth PL1 3DH, UK

O. Hoegh-Guldberg
Global Change Institute, The University of Queensland, Research Road, St Lucia, Brisbane, QLD, Australia

Introduction

Coral reefs worldwide are increasingly under threat from climate change-induced bleaching events (Hoegh-Guldberg 1999; Baker et al. 2008), ocean acidification (Hoegh-Guldberg et al. 2007), predator outbreaks (Kayal et al. 2012), and disease (Harvell et al. 1999, 2007). While we are beginning to better understand the mechanisms involved in bleaching (Douglas 2003; Weis 2008), the causative agents of many coral diseases remain unknown. Given that coral disease prevalence may be correlated with periods of stress, such as temperature anomalies (Bruno et al. 2007; Ferreira et al. 2013), it is likely that disease prevalence will increase in the future in response to climate change and other anthropogenic impacts (Harvell et al. 1999, 2007). Already, disease following bleaching has resulted in drastic declines in coral cover in the Caribbean (Miller et al. 2009). Clearly, a better understanding of the numerous identified coral diseases is critical if we are to

mitigate at least some of the degradation of reefs that is predicted to occur.

Corals of the genus *Porites* are important members of many reefs in the Indo-Pacific and are commonly affected by disease (Raymundo et al. 2005). Documented diseases of poritid corals in this region include growth anomalies (tumours; Domart-Coulon et al. 2006; Kaczmarsky and Richardson 2007; Aeby et al. 2011), *Porites* ulcerative white spot disease (PUWS; Raymundo et al. 2003), *Porites* bleaching with tissue loss (Sudek et al. 2012), and trematodiasis (Aeby 2006). The disease under study here, white patch syndrome (WPS), was first described in 2008 (Roff et al. 2008). These authors found that WPS manifested as patches of discolouration (with no associated tissue loss) on colonies of *Porites lobata* on the Great Barrier Reef (GBR). Patches were 20–100 mm in diameter, circular to oblong in shape and had distinct edges. Measurements of photosynthetic health suggested that *Symbiodinium* cells within the patches were either damaged or expelled. WPS appears to persist over long time periods on affected colonies: a monitoring programme carried out on eight colonies of *Porites* spp. displaying WPS symptoms at three reef sites on the GBR from July 2004 to January 2006 revealed temporal changes in lesion size and coverage, but lesions were present at all sampling time points on initially diseased colonies (J. Davy pers. obs.). The causative agent of WPS is currently unknown. Roff et al. (2008) noted that the macroscopically similar disease PUWS may be caused by *Vibrio* sp., however, the relationship between these two diseases is unknown.

In the current study, we set out to further characterize WPS through physiological examination and microscopic analysis. Furthermore, we attempted to identify the causative agent of this disease. A particular focus of this study was to determine whether viruses play a role in WPS. Virus-like particles (VLPs) have previously been found in tissues of thermally stressed corals (Wilson et al. 2005; Davy et al. 2006) and stressed *Symbiodinium* (Lohr et al. 2007), and have been shown to cause lysis of *Symbiodinium* cells (Wilson et al. 2001). We also have evidence of latent viral infections in numerous strains of *Symbiodinium* that can be induced through stress (unpublished data). Further evidence for a potential viral basis of coral diseases comes from the work of Vega Thurber et al. (2008), who found, through the use of metagenomics, that stress induces herpes-like viruses in *Porites compressa*. More recently, Soffer et al. (2014) showed that small circular single-stranded DNA viruses are associated with white plague disease of the coral *Montastraea annularis* in the Caribbean. With these findings in mind, we used electron microscopy to identify and enumerate viruses associated with healthy and WPS-affected poritid corals on the Great Barrier Reef.

Methods

2004–2006 Study

Physiology of white patch syndrome

Symbiont density Two samples each of visibly healthy and lesion tissue were collected from each of two colonies of *Porites lutea* showing symptoms of WPS (WPS lesion: $n = 4$; healthy: $n = 4$) on SCUBA from depths of 7–12 m at Twin Peaks, Heron Reef, GBR (23°28.346′S, 151°57.571′E), in October 2005. A corer (4.9 cm^2) attached to a power drill was used to collect the samples, which were transported back to the laboratory in plastic bags containing sea water. Coral cores were placed in a flow-through aquarium system and processed within 3 h. White patch syndrome lesion and healthy areas of each sample were separated using a Dremel^{TM} rotary cutting tool fitted with a diamond cutting disc (Bosch, Australia). Samples were placed in a small plastic bag and tissue removed using an airgun attached to a SCUBA cylinder high pressure outlet. The tissue slurry was agitated in 0.45-µm filtered sea water (FSW) and centrifuged at 4,100×*g* for 5 min at 4 °C in a sterile 50-ml centrifuge tube to pellet the algal symbionts. A 1.5 ml aliquot of the resultant supernatant was taken for determination of the host protein content (see next section). The algal pellet was resuspended in a known volume of FSW to give approximately 10^6 cells ml^{-1}. Symbiont density was determined using a haemocytometer by counting eight replicate grids for each sample. Results for analysis of symbiont density, chlorophyll *a* content, and protein content were normalized to surface area, using the aluminium foil method of Marsh (1970).

Coral tissue protein content Host protein content was determined using the supernatant of the tissue slurry described in the previous section. An aliquot of each sample was diluted as necessary with 0.2-µm FSW and the absorbance read on a UV-2450 UV−Visible spectrophotometer (Shimadzu Scientific Instruments, Columbia, USA). Protein content was calculated using absorbance at A_{235} and A_{280}, with the following formula (Whitaker and Granum 1980):

$$P = (A_{235} - A_{280}) \times 2.51 \times \mathrm{DF} \times V$$

where P = protein content (ng), DF = dilution factor, V = volume airbrushed, A_{235} = absorbance at 235 nm, and A_{280} = absorbance at 280 nm.

Spectrophotometric determination of chlorophyll a concentration Samples of *P. lutea* (WPS lesion: $n = 3$, visibly healthy: $n = 4$) for chlorophyll *a* analysis were

collected from Libby's Lair, Heron Reef (23°26.075′S, 151°56.018′E), at a depth of ~12 m, in May 2006 for chlorophyll *a* analysis. Chlorophyll *a* concentration was measured by extracting pigment from coral cores by first placing coral fragments in foil-wrapped tubes containing 10 ml methanol and then placing them on ice in a sonicating water bath (Unisonics, Manly Vale, Australia) for 10 min. Tubes were then placed at −20 °C overnight and the following day spun at 5,000×*g* for 10 min at 4 °C. The optical densities of the supernatant were measured on a Cintra UV–Visible spectrometer (GBC, Dandenong, Australia) at 750, 666, and 653 nm, with blanks between each sample. The equation given in Wellburn (1994) was used to calculate chlorophyll *a* concentration after a correction for turbidity was made:

$$\text{Chl}a = 15.65A_{666} - 7.34A_{653}$$

where Chl*a* = chlorophyll *a* concentration (μg ml^{-1}), A_{666} = absorbance at 666 nm, and A_{653} = absorbance at 653 nm.

Photophysiology of symbiodinium associated with WPS

Nine cores were taken from colonies of *Porites* spp. corals growing at approximately 6–10 m depth at North Wistari Reef (23°27.173′S, 151°53.137′E; *Porites* sp., $n = 2$ and *P. australiensis*, $n = 4$) and Harry's Bommie (23°27.631′151°S, 55.798′E; *P. lutea*, $n = 3$) in October 2005. Coral cores were maintained in flow-through sea water aquaria (80 l) at ambient temperature (25.8 °C ± 0.15; mean ±SE) under shade (<200 μmol photons m^{-2} s^{-1}) for 2 days prior to measurement of chlorophyll fluorescence. Due to the extreme difficulty of identifying poritid corals in the field, samples were not taken from colonies of a single species. However, statistical analysis showed that there was no colony effect on the fluorescence parameters measured during this analysis (data not shown), and previous researchers have considered the species *P. australiensis, P. lobata*, and *P. lutea* as the single unit 'massive *Porites*' due to the lack of perceived differences in biological characteristics between them (Done and Potts 1992). Photosynthetic efficiency of Photosystem II (PSII) was measured after 30 min of dark adaptation at dusk to ensure all reaction centres were open (Krause and Weis 1984; Jones et al. 1998). Measurements were taken across a gradient from lesion, border area, and apparently healthy areas of coral using an Imaging-PAM fluorometer (IPAM, Walz GmbH, Effeltrich, Germany) with a maxi-measuring head attachment (70 × 100 mm) to generate dark-light induction curves. While this method necessitated the harvesting of coral cores, it was otherwise ideal as it provides high resolution and the ability to assess spatial heterogeneity of variable fluorescence across the coral surface (Hill et al. 2004; Ralph et al. 2005). The minimal (F_o) and maximal (F_m) fluorescence yields were obtained through the application of a series of saturation pulses (>10,000 μmol photons m^{-2} s^{-1}) at constant LED-emitted actinic irradiance (186 μmol photons m^{-2} s^{-1}). Saturation pulses were applied at 20 s intervals to measure steady state effective quantum yield, $\Delta F/F_m'$.

Statistical analysis

The nonparametric Mann–Whitney *U* test was used when sample sizes were too small to allow for use of the independent samples *t* test or one-way ANOVA. One-way ANOVA was used to test for significant differences between variables measured with the IPAM. All statistical analysis was carried out using software package Statistica version 7 (Statsoft Inc., Oklahoma, USA). Due to logistical constraints, samples used for symbiont density and protein analyses were collected at different times and locations than those used for chlorophyll *a* and photophysiology analyses. As such, changes in these parameters could not be assessed relative to each other.

Transmission electron microscopy

Twenty-eight tissue samples were collected from colonies of *Porites* spp. at five sites around Heron Island. Samples were collected between July 2004 and January 2006, using a hammer and chisel, and consisted of diseased and visibly healthy tissue from diseased colonies, and healthy tissue from unaffected colonies. Samples were fixed in 3 % glutaraldehyde in 0.1 M sodium cacodylate buffer within 30 min of collection and post-fixed in 1 % aqueous osmium tetroxide. Fixative was removed, and samples were decalcified in 20 % EDTA in PBS at 4 °C. The EDTA solution was changed daily for up to 2 weeks. Following decalcification, samples were dehydrated through an ethanol series (50–100 %) and embedded in Epon™ resin in a PELCO BioWave microwave (PELCO International, Redding, USA) according to the manufacturer's instructions. Ultrathin sections were cut on an Ultracut T ultramicrotome (Leica Microsystems, Vienna, Austria). Sections were mounted on 200-μm mesh copper grids (ProSciTech, Townsville, Australia) and stained with 5 % (w/v) uranyl acetate in 50 % ethanol (2 min) and 1.5 % lead citrate (1 min). Grids were viewed on a JEM-1010 TEM (JEOL, Tokyo, Japan) at an acceleration voltage of 80 kV, and images were captured using the Megaview III Soft Imaging system (Olympus, Japan).

2010 Study

The 2004–2006 study provided evidence of virus-like particles (VLPs) associated with *Porites* spp. displaying

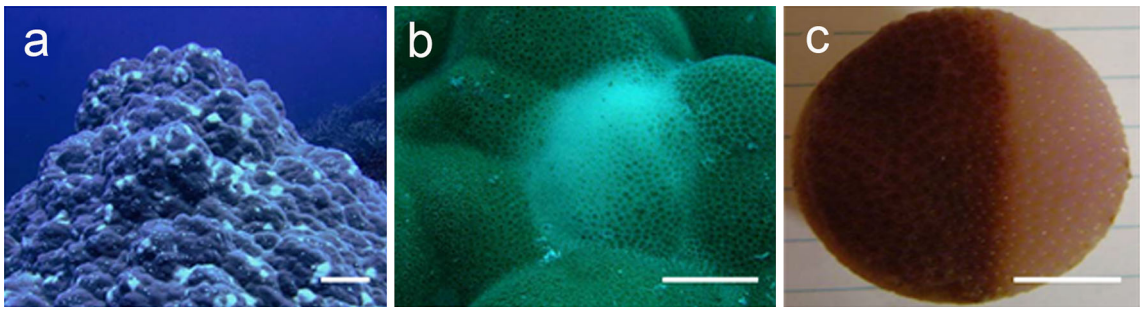

Fig. 1 Macroscopic signs of white patch syndrome. **a** Discrete, irregular white patches of varying sizes on a colony of *Porites lutea,* **b** diffuse lesions on a colony of *Porites* sp., **c** fragment of *Porites australiensis* showing distinct demarcation between healthy (*left*) and diseased tissue (*right*). *Scale bars* represent **a** 30 cm, **b** 5 cm, and **c** 3 cm

WPS. A follow-up study was therefore carried out in 2010, in order to enumerate and identify VLPs associated with the disease.

Sample collection

Tissue fragments of *P. australiensis* were collected with hammer and chisel from colonies at Harry's Bommie, Wistari, and Twin Peaks reefs, at ~6-m depth, in July 2010, at Heron Island, GBR. Samples were taken directly from WPS lesions ($n = 10$), from visibly healthy tissue ~1 cm away from the lesion ($n = 10$), and from non-diseased colonies ($n = 10$). The tissue samples were fixed in 2.5 % glutaraldehyde within 1 h of collection and refrigerated at 4 °C until processing.

Transmission electron microscopy

Glutaraldehyde-fixed tissue samples were decalcified in 0.5 M EDTA and post-fixed in 2 % osmium tetroxide. Samples were then dehydrated through an ethanol series (50–100 %) and propylene oxide, and embedded in Procure 812 resin (Proscitech, Queensland, Australia). Ultrathin sections were cut on an Ultracut T ultramicrotome (Leica Microsystems, Vienna, Austria) and were stained using 2 % aqueous uranyl acetate and Reynold's lead citrate. Sections were viewed on a Philips CM-100 transmission electron microscope operated at 80 kV. Five samples of each sample type (healthy, diseased, and 1 cm from lesion) were analysed. In each case, 30 fields of view at 24,500× magnification were examined for the presence of VLPs in *Symbiodinium* cells and gastrodermal and epidermal tissues. Observed VLPs were sorted into two morphological groups (icosahedral and filamentous) and four size classes (0–50, 51–100, 101–150, >150 nm). Nonparametric analyses of variance were carried out using PASW Statistics 18 (SPSS Inc., Chicago, USA) to determine any difference in virus abundance between samples.

Results

Macroscopic characteristics of WPS

During the 2004–2006 study, macroscopic characteristics of WPS were analysed prior to sampling. WPS manifested as discrete to diffuse multi-focal white lesions that ranged in size from <1 cm^2 to approximately 25 cm^2 (Fig. 1). Lesions were more commonly irregular in shape but occasionally ovoid. Edges of lesions were generally distinct and smooth, the coral surface texture smooth, and the whole polyp showed colour loss. Lesions were not limited to the upper, sunlit surfaces of corals but distributed across the colony and the host range of WPS appeared to be limited to the massive poritid species *P. australiensis, P. lobata*, and *P. lutea*. The lack of skeletal destruction and the prolonged persistence of some lesions suggested that they were not predation scars or fish bites. A qualitative estimate of maximum lesion coverage on any colony affected by WPS during the course of this study was 30 % of total colony surface area, seen on a colony at Harry's Bommie (23°27.631′151°S, 55.798′E) at a depth of 12 m.

Physiology of WPS

Symbiont density, chlorophyll a concentration, and host protein content

The population density of *Symbiodinium* in tissue affected by WPS was significantly lower than in the healthy tissue immediately adjacent to lesions (Mann–Whitney U, $p = 0.021$), with 40 % less symbionts. WPS lesion tissue contained $0.96 \pm 0.22 \times 10^6$ *Symbiodinium* cells cm^{-2} (mean ± SE), while visibly healthy tissue contained $2.66 \pm 0.46 \times 10^6$ *Symbiodinium* cells cm^{-2}. There was also a significant difference in chlorophyll *a* content (Mann–Whitney U, $p = 0.049$), with lesion tissue having a lower amount of chlorophyll *a* (0.65 ± 0.06 μg cm^{-2}; mean ± SE)

than surrounding healthy tissue (2.03 ± 0.13 μg cm^{-2}). The host tissue biomass (expressed as protein per unit surface area) was higher in lesions, with 7.81 ± 0.86 ng cm^{-2} (mean ± SE) compared to the healthy tissue content of 5.24 ± 0.82 ng cm^{-2}, but this difference was not significant (Mann–Whitney U, $p = 0.157$).

Photophysiology of corals

Data for all three sampled colonies were pooled as analysis showed that there was no difference in the dark-adapted maximum quantum yield (F_v/F_m; one-way ANOVA, $F_{2,24} = 1.758$, $p = 0.19$) or non-photochemical quenching (NPQ; one-way ANOVA, $F_{2,24} = 0.320$, $p = 0.74$) between the colonies.

Minimum fluorescence, F, indicated a lower level of chlorophyll *a* content within the lesion, which is in agreement with the spectrometry readings of this parameter. Maximum fluorescence was also lower, resulting in an F_v/F_m value of 0.584 ± 0.007, which was lower than was seen in the border (0.6 ± 0.005) and healthy tissue (0.596 ± 0.005), but not significantly so (one-way ANOVA, $F_{2,24} = 1.76$, $p = 0.1938$). There was also no significant difference between the level of NPQ for the light level chosen for the PAM measurements (186 μmol photons m^{-2} s^{-1}) (one-way ANOVA, $F_{2,15} = 0.32$, $p = 0.729$). The effective quantum yield ($\Delta F/F_m'$) during the course of the dark-light induction curve was lower in the lesions than in the border and healthy regions (0.3295 ± 0.012 vs. 0.3889 ± 0.021 and 0.3767 ± 0.019; respectively; mean ± SE), but analysis showed that this was not a significant difference (one-way ANOVA, $F_{2,25} = 3.16$, $p = 0.071$). The difference in photosynthetic efficiency between WPS, border region and healthy tissue is also illustrated in Fig. 2. In sample 3011a (black line), there was a mild elevation in effective quantum yield at the border of the healthy and lesion tissue, followed by a rapid decline that corresponded to the region of lesion tissue. This borderline elevation was not apparent in the trace of the second sample (blue line), but the value of effective quantum yield was lower in the lesion tissue.

Transmission electron microscopy

In both the 2004–2006 and 2010 studies, host tissue was found to remain relatively intact within the disease lesion. Although not quantified, necrosis (characterized by chromatin condensation, cell/organelle swelling, and vacuolization of the cytoplasm) and apoptosis (characterized by cell shrinkage, chromatin condensation, and formation of apoptotic bodies) of coral and *Symbiodinium* cells appeared to be occurring at similar rates in all samples (see Fig. 3a, b for examples). Little cell debris was observed among

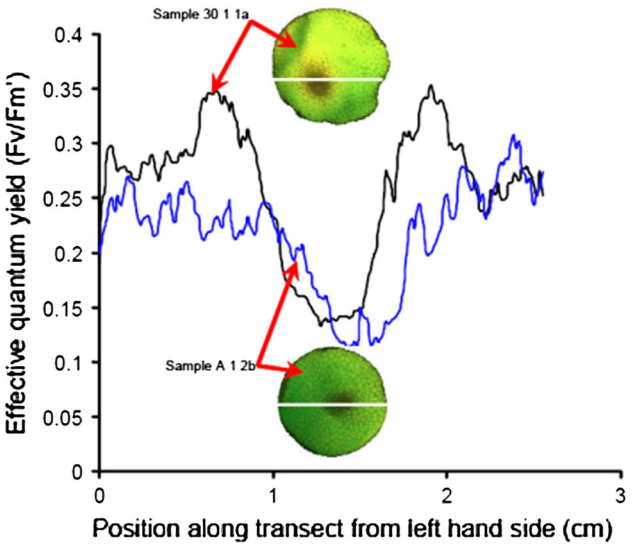

Fig. 2 Photosynthetic efficiency of *Porites* spp. corals with white patch syndrome. Plots show changes in effective quantum yield ($\Delta F_v/F_m'$) following 10 s of light exposure at >10,000 μmol m^{-2} s^{-1} along a transect through visibly healthy tissue and lesions (*left* to *right*) of two representative cores (A12b = *P. australiensis*; 3011a = *P. lutea*). *Inset* pictures show the false colour IPAM images of the effective quantum yield (a single transect is plotted—represented by *white line*)

surrounding cells or in the gastric cavity of the host, suggesting that necrosis was not occurring extensively in healthy or diseased tissues. One notable difference among sample types was the presence of 'holes' in the gastrodermal preparations of diseased colonies, presumably caused by loss of *Symbiodinium* cells (Fig. 3d). Although not quantified, these tissue holes were relatively rare in healthy tissue samples. Numerous bacterial aggregates were seen in both healthy and diseased samples, with no apparent correlation with disease state (Fig. 3e).

Numerous virus-like particles (VLPs) were observed in all samples and cell types (epidermis, gastrodermis, and *Symbiodinium* cells). In the samples collected between 2004 and 2006, VLPs consisted of a single icosahedral morphotype, 90–120 nm in diameter (Fig. 4a). VLPs showed no evidence of an envelope, tail, or other appendages. These particles were only found within diseased coral tissue and visibly healthy coral tissue from diseased colonies (i.e. they were never seen in tissue from healthy colonies or inside *Symbiodinium* cells). VLPs often formed large aggregates within the cytoplasm of coral gastrodermis and epidermis cells (Fig. 4a), as well as being found as individual particles scattered throughout these tissues. In the 2010 study, icosahedral VLPs ranging in size from ~20–200 nm were seen in coral tissues, while *Symbiodinium* VLPs consisted mostly of filamentous VLPs up to 100 nm in length, with icosahedral VLPS also present in some samples (Fig. 5). All VLPs appeared to be non-

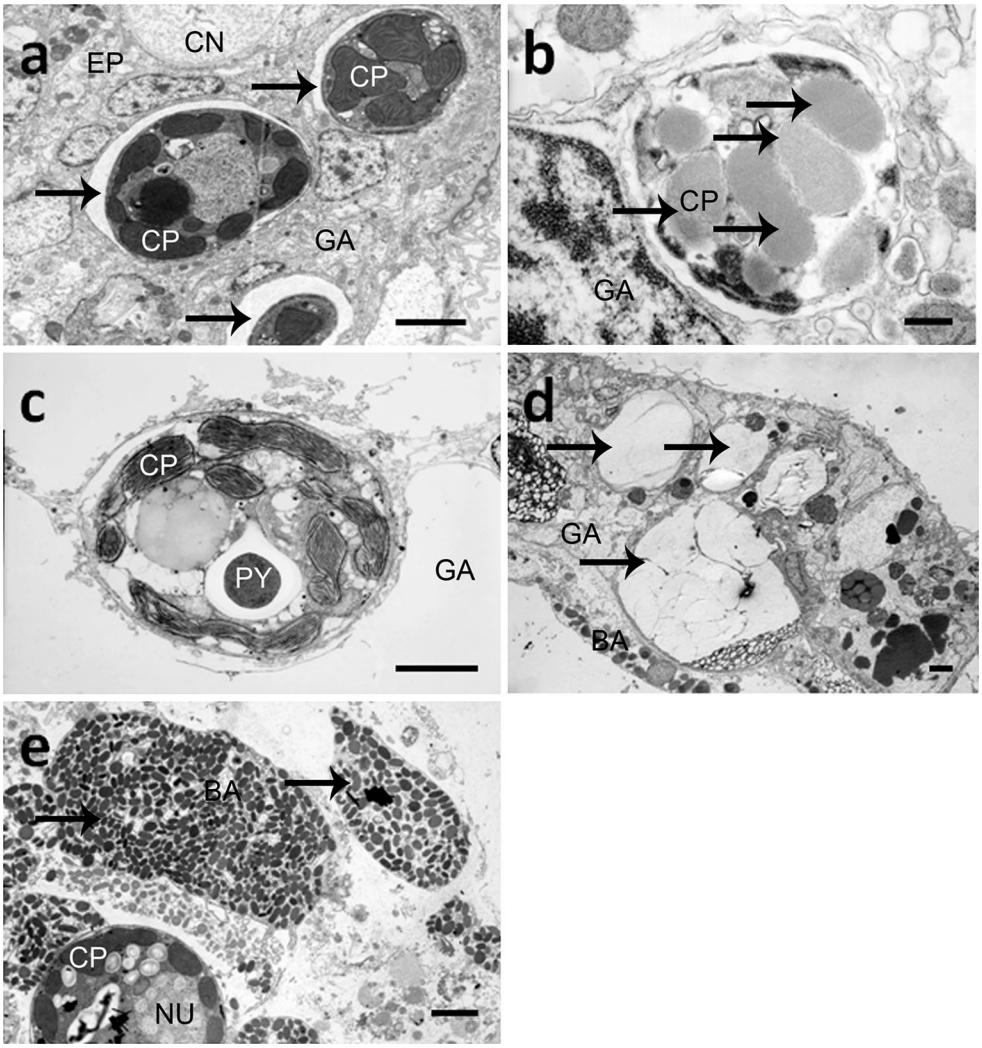

Fig. 3 Transmission electron micrographs of *Porites* spp. coral and *Symbiodinium* cells. **a** *Symbiodinium* cells in early stage of apoptosis from tissue 1 cm away from WPS lesion in *P. australiensis*; note cell shrinkage (*arrows*), **b** necrotic *Symbiodinium* cell from lesion tissue in *P. lutea*; *arrows* indicate swollen chloroplasts, **c** *Symbiodinium* cells being released into gastrodermis within WPS lesion in *P. lutea*, **d** tissue holes (*arrows*) resulting from *Symbiodinium* loss in tissue 1 cm away from lesion in *P. australiensis*, **e** bacterial aggregates (*arrows*) in a healthy colony of *P. australiensis. Scale bars* are 2 μm. BA: bacterial aggregate, *CN* cnidocyte, *CP* chloroplast, *EP* epidermis, *GA* gastrodermis, *NU* nucleus, *PY* pyrenoid

enveloped, without tails or other appendages (Fig. 4a, b). It should be noted though that, while the TEM used in this study is capable of resolving viral envelopes and appendages, the possibility remains that envelopes or appendages were destroyed during sample decalcification or dehydration. Nonparametric analysis of variance revealed no significant difference in overall VLP abundance among sample types (Kruskal–Wallis, $p = 0.101$). Likewise, at the level of tissue/cell type (epidermis, gastrodermis, and *Symbiodinium*), there was no significant difference in overall VLP abundance (Kruskal–Wallis, $p = 0.06$) or abundance of individual VLP size/morphology classes among sample types ($p > 0.05$ for all comparisons). There was, however, a significant difference in overall abundance of small (<50 nm diameter) icosahedral VLPs among sample types (Kruskal–Wallis, $p = 0.021$), with ~3 times as many seen in tissue collected 1 cm away from disease lesions than in healthy or diseased tissues. Also, even though not statistically significant (Kruskal–Wallis, $p = 0.218$), there was an apparent increase in filamentous VLPs > 50 nm in length in *Symbiodinium* cells from diseased colonies (lesion: ~400 %, 1 cm: ~600 % increase). Abundances of VLP morphotypes observed in the different sample and tissue types are presented in Fig. 5.

Discussion

In this study, we examined the physiology of *Porites* spp. corals with white patch syndrome and characterized viruses

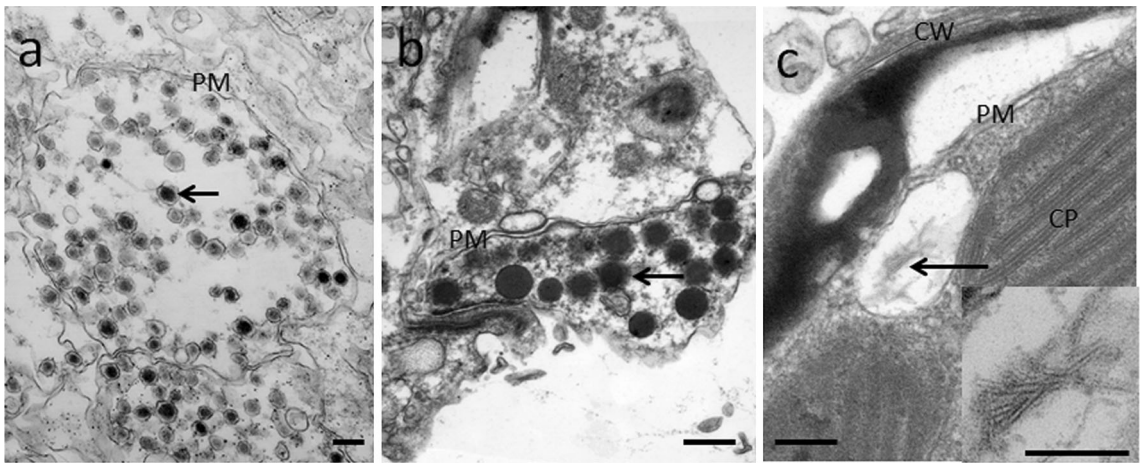

Fig. 4 Transmission electron micrographs of virus-like particles (VLPs) from diseased *Porites* spp. colonies. **a** VLPs in diseased tissues of *Porites* spp. (*arrows*), **b** VLPs in epidermis of *Porites australiensis* WPS lesion, **c** filamentous VLPs in *Symbiodinium* from tissue 1 cm away from WPS lesion in *P. australiensis* (*inset*: increased magnification of VLPs). *Scale bars* are 200 nm. PM: plasma membrane, *CW* cell wall, *CP* chloroplast

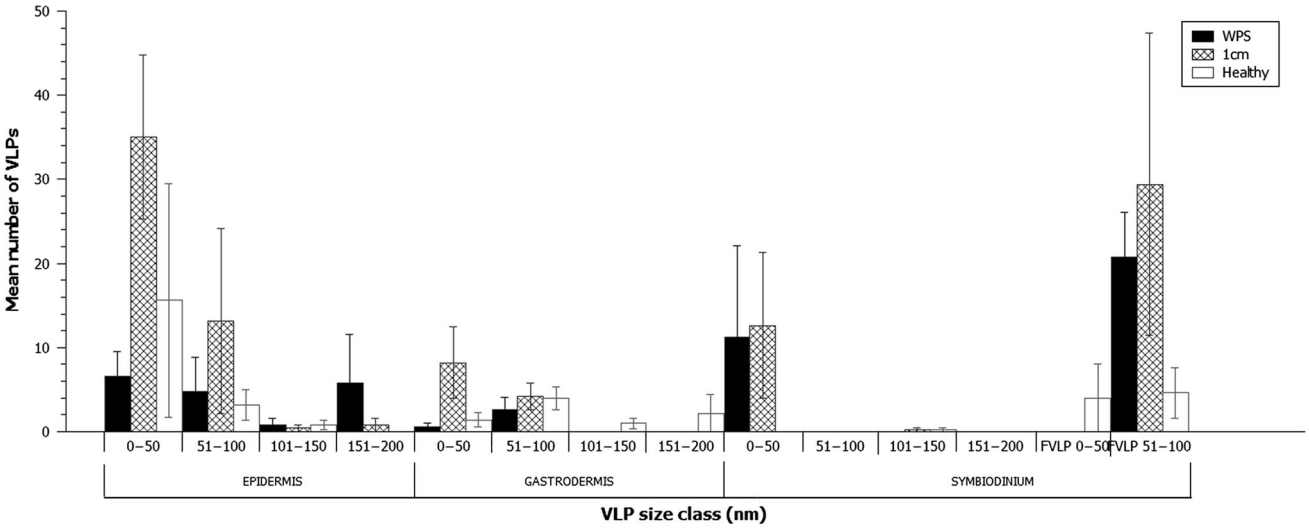

Fig. 5 Abundance of VLP morphotypes found in *Porites australiensis* in the 2010 study. *Black bars* represent WPS lesion tissue, *shaded bars* represent tissue 1 cm away from lesion, and *white bars* represent samples from healthy colonies. *Error bars* represent standard error

associated with the disease. Physiological analysis showed a significant decrease in *Symbiodinium* cell density in WPS lesions, while host tissue biomass (protein per unit biomass) was apparently unaffected. This was consistent with measurements of photosynthetic health, which showed that tissue within the WPS lesions was less photosynthetically efficient than surrounding tissue. These results indicate that *Symbiodinium* cells are lost from diseased tissues, but that host tissue remains intact. TEM analysis confirmed this; host tissues from diseased samples were not visibly different from tissue samples from healthy colonies, but there was evidence of *Symbiodinium* cell loss. This is in line with the findings of Roff et al. (2008), who also found decreased photosynthetic health in WPS lesions. The loss of *Symbiodinium* cells seen here is also consistent with *Symbiodinium* cell loss observed in *Montastraea* spp. corals with yellow blotch/band disease (Cervino et al. 2004). Additionally, there was no correlation between disease state and sea water temperature or season (ESM, Electronic Supplementary Material, Fig. S1, S2, S3), providing further evidence that WPS is a true disease, rather than conventional thermally induced coral bleaching. Despite the apparent lack of environmental stressors seen here, further study is required to determine whether the causative agent of WPS requires a compromised host for successful infection.

Bacterial abundance in the corals studied here was patchy and did not appear to differ with disease state,

whereas abundance of small VLPs was significantly higher in tissue samples collected 1 cm away from WPS lesions. The increased VLP abundance adjacent to lesions relative to within the lesions themselves may be a result of VLP release occurring as the host cells are compromised or lost from the tissue. Although not significantly different, there was also an apparent increase in abundance of filamentous VLPs in *Symbiodinium* cells from diseased colonies, compared to samples from healthy colonies. While the icosahedral VLPs seen in coral tissues are difficult to identify based solely on morphology, they resemble VLPs previously found in a range of coral species (Wilson et al. 2005; Davy et al. 2006; Bettarel et al. 2013). Davy et al. (2006) provided evidence that such VLPs are capable of infecting and lysing healthy *Symbiodinium* cells isolated from corals.

In the current study, small (<50 nm diameter) VLPs showed increased abundance in both the *Symbiodinium* and coral cells of diseased samples, suggesting that they could be causing *Symbiodinium* cell lysis directly and/or compromising the coral cells and causing a breakdown in the coral–*Symbiodinium* symbiosis. Virus-like particles in this size range have been observed previously in dinoflagellates (Franca 1976; Soyer 1978), but only one dinoflagellate-infecting virus of this size has so far been characterized. *Heterocapsa circularisquama* RNA virus (HcRNAV) is a positive-stranded RNA virus which is capable of rapidly lysing its dinoflagellate hosts (Tomaru et al. 2004) and is considered an important factor in *H. circularisquama* bloom termination (Nagasaki et al. 2004; Tomaru and Nagasaki 2004). Similarly, studies of viruses within coral cells have until recently been restricted to electron microscopy examination, making accurate identification difficult. Furthermore, as shown in two recent studies using metagenomics and metatranscriptomics approaches (Vega Thurber et al. 2008; Correa et al. 2012), a vast range of viruses associate with coral colonies, making it difficult to speculate on the potential identities or modes of action of the putative viruses seen here. With that said, the recent work of Soffer et al. (2014) revealed small circular single-stranded DNA viruses (SCSDVs) associated with white plague disease in *Montastraea annularis*. This virus group includes the families *Circoviridae*, *Geminiviridae*, and *Nanoviridae*, all of which are small, icosahedral viruses, and could potentially be phylogenetically similar to the VLPs seen here.

The filamentous VLPs seen here in *Symbiodinium* cells resemble those seen in stressed cultured *Symbiodinium* cells by Lohr et al. (2007) and by the authors of this paper in several cultured strains of *Symbiodinium* sp. following stress (unpublished data). Lohr et al. (2007) hypothesized that these filamentous VLPs were members of the *Closteroviridae*, but these VLPs also resemble other virus groups such as the *Inoviridae* and *Flexiviridae*. Without higher resolution molecular analysis, it is not possible to confirm to which family they belong. If these filamentous VLPs are proven to indeed be viruses, it is possible that they are causing loss of *Symbiodinium* cells in WPS-infected corals either through *Symbiodinium* cell lysis or by impairing *Symbiodinium* cell function and causing a breakdown in the coral–algal symbiosis.

We have shown here that WPS is a disease affecting *Symbiodinium* in several species of poritid corals on the Great Barrier Reef. *Symbiodinium* cells are lost without any noticeable damage to the surrounding coral tissue, resulting in the bleached appearance of the disease lesion. There is evidence that viruses might play a role in the loss of *Symbiodinium*, although the trigger for viral induction has not yet been identified. Future work should focus on confirming the viral basis of the disease and determining whether it is a latent or opportunistic infection. If WPS is indeed confirmed as a viral disease, the next step will be to identify the environmental factors causing stress to these corals and subsequently inducing viral lysis or allowing infection. The role of viral vectors could also be explored, as the patchy nature of WPS suggests that a vector such as a corallivorous animal may be transferring the putative pathogens to the coral.

Acknowledgments The authors wish to thank Dr. Paul Fisher for coral sample collection, Dr. St.John Wakefield for providing access to TEM facilities, and David Flynn for assistance with TEM sample preparation. We also thank two anonymous reviewers for their helpful comments on this manuscript. SAL was supported by a NZ Tertiary Education Commission Top Achiever Doctoral Scholarship. WHW was supported in part by National Science Foundation grant OCE0851255.

References

Aeby GS (2006) Baseline levels of coral disease in the Northwestern Hawaiian Islands. Atoll Res Bull 543:471–488

Aeby GS, Williams GJ, Franklin EC, Haapkyla J, Harvell CD, Neale S, Page CA, Raymundo L, Vargas-Ángel B, Willis BL, Work TM, Davy SK (2011) Growth anomalies on the coral genera *Acropora* and *Porites* are strongly associated with host density and human population size across the Indo-Pacific. PLoS One 6:e16887

Baker AC, Glynn PW, Riegl B (2008) Climate change and coral reef bleaching: An ecological assessment of long-term impacts, recovery trends and future outlook. Estuar Coast Shelf Sci 80:435–471

Bettarel Y, Thuy NT, Huy TQ, Hoang PK, Bouvier T (2013) Observation of virus-like particles in thin sections of the bleaching scleractinian coral *Acropora cytherea*. J Mar Biol Assoc UK 93:909–912

Bruno JF, Selig ER, Casey KS, Page CA, Willis BL, Harvell CD, Sweatman H, Melendy AM (2007) Thermal stress and coral cover as drivers of coral disease outbreaks. PLoS Biol 5:e124

Cervino JM, Hayes R, Goreau TJ, Smith GW (2004) Zooxanthellae regulation in Yellow Blotch/Band and other coral diseases

contrasted with temperature related bleaching: in situ destruction vs expulsion. Symbiosis 37:63–85

Correa AMS, Welsh RM, Vega Thurber RL (2012) Unique nucleocytoplasmic dsDNA and +ssRNA viruses are associated with the dinoflagellate endosymbionts of corals. ISME J 7:13–27

Davy SK, Burchett SG, Dale AL, Davies P, Davy JE, Muncke C, Hoegh-Guldberg O, Wilson WH (2006) Viruses: agents of coral disease? Dis Aquat Org 69:101–110

Domart-Coulon IJ, Traylor-Knowles N, Peters E, Elbert D, Downs CA, Price K, Stubbes J, McLaughlin S, Cox E, Aeby G, Brown PR, Ostrander GK (2006) Comprehensive characterization of skeletal tissue growth anomalies of the finger coral *Porites compressa*. Coral Reefs 25:531–543

Done TJ, Potts DC (1992) Influences of habitat and natural disturbances on contributions of massive *Porites* corals to reef communities. Mar Biol 114:479–493

Douglas AE (2003) Coral bleaching: How and why? Mar Pollut Bull 46:385–392

Ferreira BP, Costa MBSF, Coxey MS, Gaspar ALB, Veleda D, Araujo M (2013) The effects of sea surface temperature anomalies on oceanic coral reef systems in the southwestern tropical Atlantic. Coral Reefs 32:441–454

Franca S (1976) On the presence of virus-like particles in the dinoflagellate *Gyrodinium resplendens* (Hulburt). Protistologica 12:425–430

Harvell CD, Jordan-Dahlgren E, Merkel S, Rosenberg E, Raymundo L, Smith G, Weil E, Willis B (2007) Coral disease, environmental drivers, and the balance between coral and microbial associates. Oceanography 20:172–195

Harvell CD, Kim K, Burkholder JM, Colwell RR, Epstein PR, Grimes DJ, Hofmann EE, Lipp EK, Osterhaus ADME, Overstreet RM, Porter JW, Smith GW, Vasta GR (1999) Emerging marine diseases - climate links and anthropogenic factors. Science 285:1505–1510

Hill R, Schreiber U, Gademann R, Larkum AWD, Kuhl M, Ralph PJ (2004) Spatial heterogeneity of photosynthesis and the effect of temperature-induced bleaching conditions in three species of corals. Mar Biol 144:633–640

Hoegh-Guldberg O (1999) Climate change, coral bleaching and the future of the world's coral reefs. Mar Freshw Res 50:839–866

Hoegh-Guldberg O, Mumby PJ, Hooten AJ, Steneck RS, Greenfield P, Gomez E, Harvell CD, Sale PF, Edwards AJ, Caldeira K, Knowlton N, Eakin CM, Iglesias-Prieto R, Muthiga N, Bradbury RH, Dubi A, Hatziolos ME (2007) Coral reefs under rapid climate change and ocean acidification. Science 318:1737–1742

Jones RJ, Hoegh-Guldberg O, Larkum AWD, Schreiber U (1998) Temperature-induced bleaching of corals begins with impairment of the CO_2 fixation mechanism in zooxanthellae. Plant Cell Environ 21:1219–1230

Kaczmarsky L, Richardson LL (2007) Transmission of growth anomalies between Indo-Pacific *Porites* corals. J Invertebr Pathol 94:218–221

Kayal M, Vercelloni J, Lison de Loma T, Bosserelle P, Chancerelle Y, Geoffroy S, Stievenart C, Michonneau F, Penin L, Planes S, Adjeroud M (2012) Predator Crown-of-Thorns Starfish (*Acanthaster planci*) outbreak, mass mortality of corals, and cascading effects on reef fish and benthic communities. PLoS One 7:e47363

Krause GH, Weis E (1984) Chlorophyll fluorescence as a tool in plant physiology. 2. Interpretation of fluorescence signals. Photosynth Res 5:139–157

Lohr J, Munn CB, Wilson WH (2007) Characterization of a latent virus-like infection of symbiotic zooxanthellae. Appl Environ Microbiol 73:2976–2981

Marsh JAJ (1970) Primary productivity of reef-building calcareous algae. Ecology 51:255–263

Miller J, Muller E, Rogers C, Waara R, Atkinson A, Whelan KRT, Patterson M, Witcher B (2009) Coral disease following massive bleaching in 2005 causes 60% decline in coral cover on reefs in the US Virgin Islands. Coral Reefs 28:925–937

Nagasaki K, Tomaru Y, Nakanishi K, Katanozaka N, Yamaguchi M (2004) Dynamics of *Heterocapsa circularisquama* (Dinophyceae) and its viruses in Ago Bay, Japan. Aquat Microb Ecol 34:219–226

Ralph PJ, Schreiber U, Gademann R, Kuhl M, Larkum AWD (2005) Coral photobiology studied with a new imaging pulse amplitude modulated fluorometer. J Phycol 41:335–342

Raymundo LJ, Harvell CD, Reynolds T (2003) *Porites* ulcerative white spot disease: description, prevalence, and host range of a new coral disease affecting Indo-Pacific Reefs. Dis Aquat Org 56:95–104

Raymundo LJ, Rosell KB, Reboton CT, Kaczmarsky L (2005) Coral diseases on Philippine reefs: genus *Porites* is a dominant host. Dis Aquat Org 64:181–191

Roff G, Ulstrup KE, Fine M, Ralph PJ, Hoegh-Guldberg O (2008) Spatial heterogeneity of photosynthetic activity within diseased corals from the Great Barrier Reef. J Phycol 44:526–538

Soffer N, Brandt ME, Correa AMS, Smith TB, Vega Thurber R (2014) Potential role of viruses in white plague coral disease. ISME J 8:271–283

Soyer M (1978) Particules de type viral et filaments trichocystoides chez les dinoflagellés. Protistologica 14:53–58

Sudek M, Work TM, Aeby GS, Davy SK (2012) Histological observations in the Hawaiian reef coral, *Porites compressa*, affected by *Porites* bleaching with tissue loss. J Invertebr Pathol 111:121–125

Tomaru Y, Nagasaki K (2004) Widespread occurrence of viruses lytic to the bivalve-killing dinoflagellate *Heterocapsa circularisquama* along the western coast of Japan. Plankton Biol Ecol 51:1–6

Tomaru Y, Katanozaka N, Nishida K, Shirai Y, Tarutani K, Yamaguchi M, Nagasaki K (2004) Isolation and characterization of two distinct types of HcRNAV, a single-stranded RNA virus infecting the bivalve-killing microalga *Heterocapsa circularisquama*. Aquat Microb Ecol 34:207–218

Vega Thurber RL, Barott KL, Hall D, Liu H, Rodriguez-Mueller B, Desnues C, Edwards RA, Haynes M, Angly FE, Wegley L, Rohwer F (2008) Metagenomic analysis indicates that stressors induce production of herpes-like viruses in the coral *Porites compressa*. Proc Natl Acad Sci USA 105:18413–18418

Weis VM (2008) Cellular mechanisms of Cnidarian bleaching: stress causes the collapse of symbiosis. J Exp Biol 211:3059–3066

Wellburn AR (1994) The spectral determination of chlorophyll *a* and chlorophyll *b*, as well as total carotenoids, using various solvents with spectrophotometers of different resolution. J Plant Physiol 144:307–313

Whitaker JR, Granum PE (1980) An absolute method for protein determination based on difference in absorbance at 235 and 280 nm. Anal Biochem 109:156–159

Wilson WH, Francis I, Ryan K, Davy SK (2001) Temperature induction of viruses in symbiotic dinoflagellates. Aquat Microb Ecol 25:99–102

Wilson WH, Dale AL, Davy JE, Davy SK (2005) An enemy within? Observations of virus-like particles in reef corals. Coral Reefs 24:145–148